Supplementary Information

Conformational Flexibility of Metazoan Fatty Acid Synthase Enables Catalysis

Edward J. Brignole[1], Stuart Smith[2], Francisco J. Asturias[1,3]

[1]Department of Cell Biology, The Scripps Research Institute, 10550 N. Torrey Pines Rd., La Jolla, CA 92037
[2]Children's Hospital Oakland Research Institute, 5700 Martin Luther King Jr Way, Oakland, CA 94609

[3]Corresponding author, Contact information: asturias@scripps.edu

SUPPLEMENTARY RESULTS

Localization of the previously unidentified ACP and TE domains. A ~30-kDa density was apparent in front of a closed FAS reaction chamber in several RCT reconstructions (**Fig. 3**, structures #706 and #823). The size and location of such density strongly suggest that it should correspond to the TE domain, the only catalytic domain not yet accommodated by our interpretation of the EM 3D reconstructions (**Supplementary Fig. 1a,b**). By contrast, smaller isolated densities were apparent in the opposite, more opened reaction chamber of these structures as well as within and around the reaction chambers of other 3D structures that likely result from mobile ACP and TE in that vicinity. Presumably the reduced mobility of the TE domain in the Δ22-FAS mutant[1] and its exclusion from the closed reaction chamber resulted in this clearly defined density in some 3D reconstructions. The presumed TE density was less apparent in corresponding 2D class averages (**Fig. 3**), possibly because overlap with other domains obscured its detection in projection.

Some 2D class averages exhibit blurred densities and high variance within the open reaction chamber, which could also indicate the presence of the elusive TE domain (**Supplementary Fig. 1c-f**). To investigate this possibility a large number of images of the Δ22 mutant that had been captured in the presence of substrates were classified, since the shortened linker in this mutant is known to restrict mobility of the TE domain[1]. 2D classification of FAS images that had been sorted into groups with homogenous overall conformation revealed, within the open reaction chambers, a globular density of variable position with a mass approximating that of the ~30-kDa TE domain (**Supplementary Fig. 1k**). When the chambers were roughly equal in size, this density was somewhat less distinct possibly due to overlap with the MAT domain (**Supplementary Fig. 1m,n**). Only small densities of variable position were apparent when the reaction chamber was closed (**Supplementary Fig. 1l**).

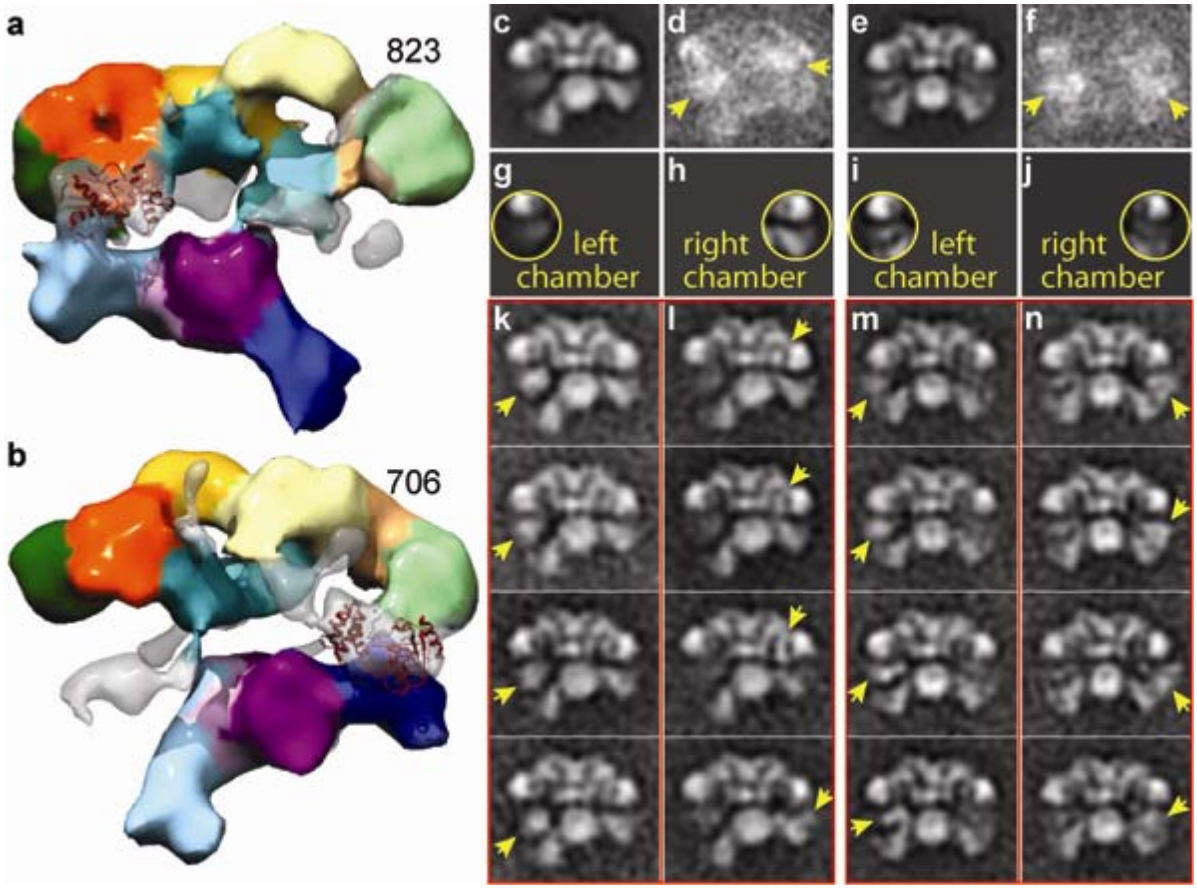

Supplementary Figure 1 TE domain can access the open reaction chambers. An atomic structure of the TE domain[2] (red ribbons; PDB: 1xkt) was fitted into density located beside the closed reaction chamber that was apparent in several of the RCT reconstructions. 3D structures from classes with 823 and 706 particles are shown (a and b, respectively; see also Fig. 3). To define more clearly TE density within the open reaction chamber, classes of Δ22-FAS particle images recorded in the presence of substrates were targeted for further classification. Class averages (c and e; also identified by asterisks in Supplementary Fig. 3) frequently contained faint blurred densities within the reaction chambers accompanied by high local pixel density variance (d and f, indicated by yellow arrows). Particle images within each class were subclassified by statistical analysis focusing on a circular region that includes each reaction chamber (g-j, yellow circles). The TE domain can be readily identified in subclass averages with open (k) and partially open (m and n) reaction chambers, but only smaller densities could be detected when chamber was closed (l). Extra densities are identified by yellow arrows.

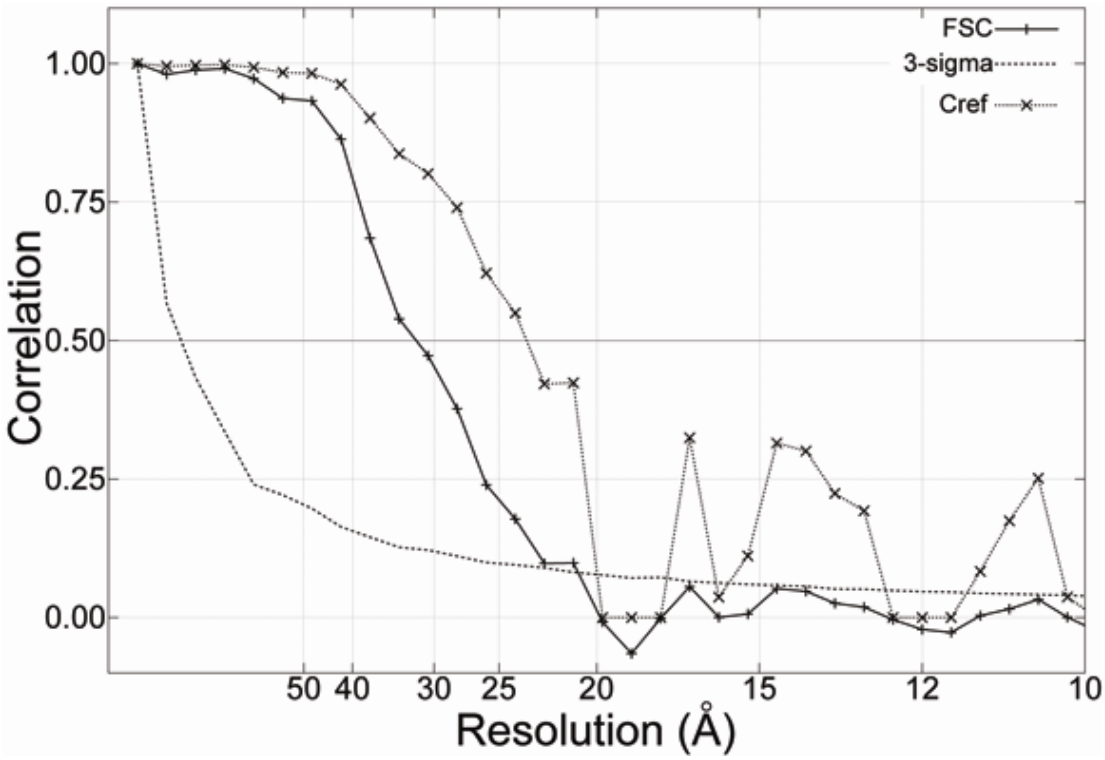

Supplementary Figure 2 3D reconstructions of negatively stained FAS achieve ~30 Å resolution. Fourier shell correlation (FSC) plot was calculated for the RCT structure of class #888 (see also Fig. 3) and results from other structures were comparable. Resolution at 0.5 correlation using FSC and Cref criterion is 32 Å and 24 Å, respectively[3]. Cref criterion may reflect the resolution more accurately in this case since the 3D reconstructions were calculated from a small number of particles and correlation was determined by splitting these data into two groups.

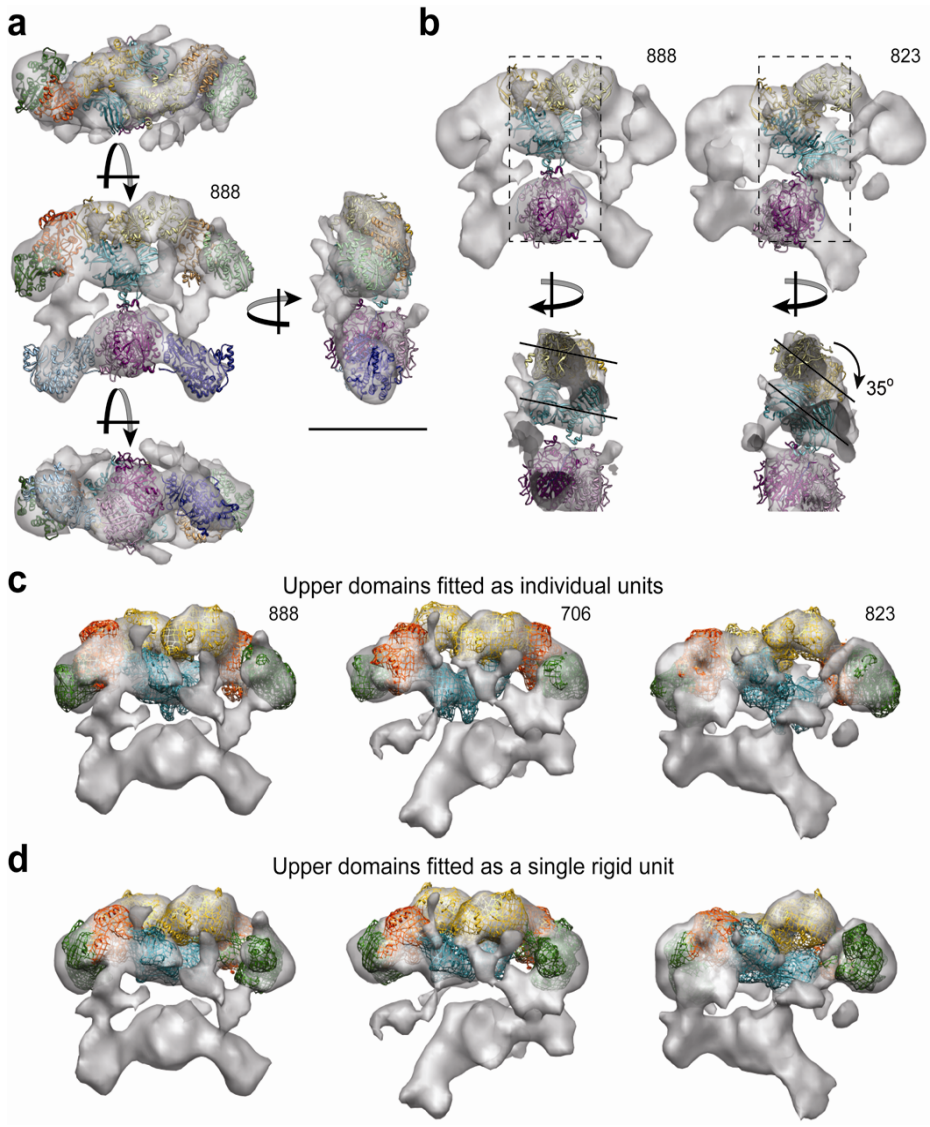

Supplementary Figure 3 FAS is well preserved in negative stain and domains can reliably be fitted into the resulting RCT reconstructions. (a) Domains fitted into the FAS structures demonstrate that FAS is resistant to deformations that commonly result from preservation in stain. (b) Fitting of the DH and ER domains into the roughly symmetrical FAS conformation (also shown in a) and a FAS reconstruction with asymmetrically arranged β-carbon processing domains illustrates the repositioning of the DH and ER dimers to form an opening in the right half of upper portion. (c,d) Rearrangement of domains within the upper portion of the structure is required to explain the opening between the DH, ER, and KR domains that is apparent in some EM reconstructions. Fitting of the upper domains of the FAS crystal structure[4] (PDB: 2vz9) as a rigid unit can readily account for the density distribution in the most symmetric EM structure (d, left panel). Fitting of individual domains to this symmetric structure (#888) only results in minor improvements (c, left panel). However, for EM reconstructions with an asymmetric upper portion (#706 and #823) rigid fitting of the corresponding domains of the crystal structure cannot account for the density distribution in the EM maps (d, middle and right panels). Whereas the separation between DH, ER, and KR domains is the same (and barely apparent) on both sides of the X-ray structure, an opening as large as ~20 Å in diameter is observed on one side of the EM reconstructions but not the other. Repositioning of individual domains of the X-ray structure is essential to explain the asymmetry observed in the EM reconstructions (c, middle and right panels). Scale bar in a represents 100 Å.

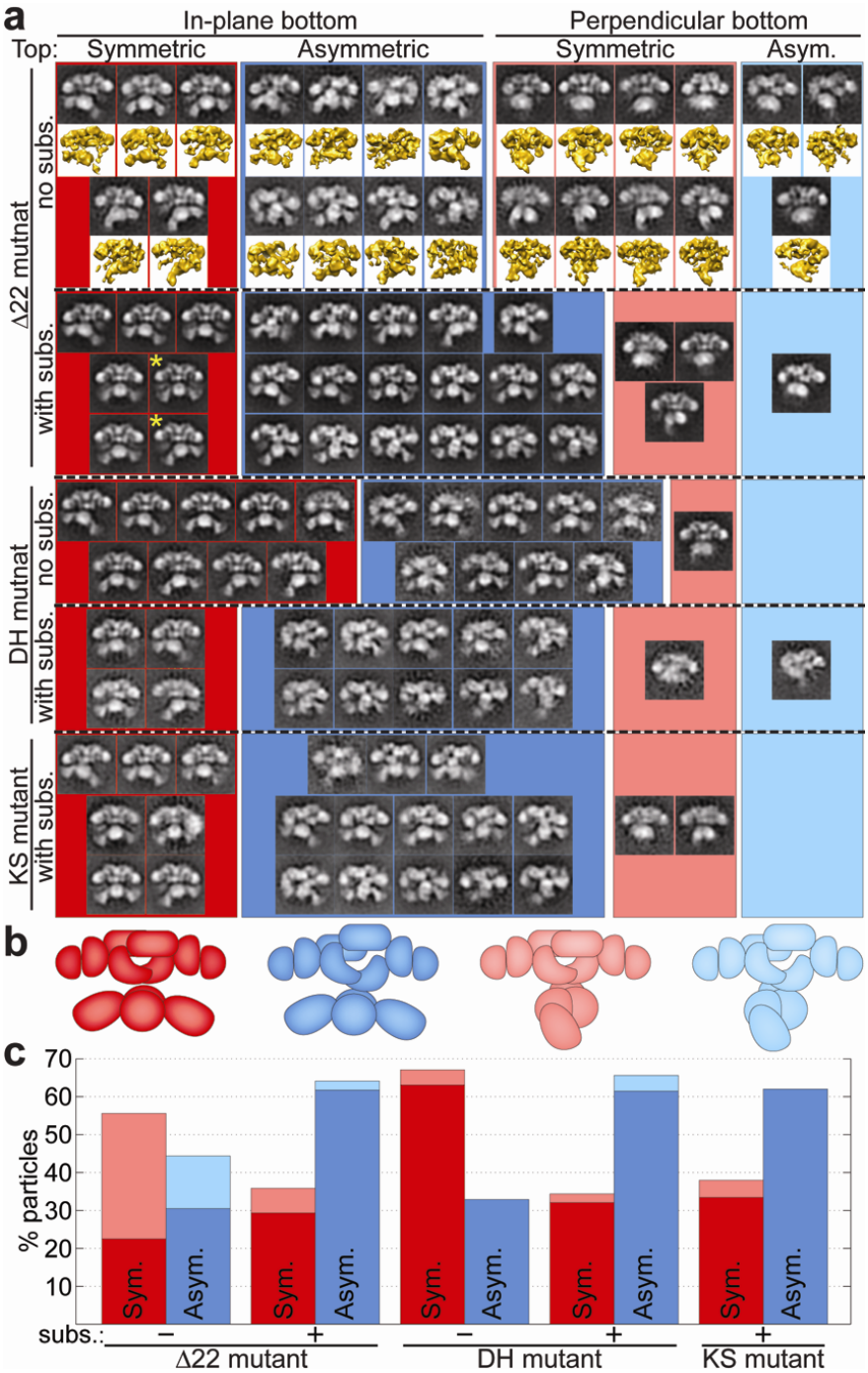

Supplementary Figure 4 Addition of substrates induces a shift in the distribution of conformations to the in-plane, asymmetric arrangement. (a) Particle images of FAS mutants in the presence and absence of substrates were aligned and classified, each preparation as an independent data set, into 30 groups. Classes were categorized based on conformation of top portion (symmetric in red, asymmetric in blue) and bottom portion (perpendicular with faded colors, in-plane with bright colors) while classes of misaligned particles were discarded (not shown). Yellow stars denote classes that were selected for further analysis of densities that likely represent the TE domain (see Supplementary Fig. 1). (b) Cartoon representation of each conformation colored as in a. (c) Addition of substrates increases the proportion of particles that have the loading/condensing domains of the lower portion in-plane with the asymmetrically arranged β-carbon processing domains of the upper portion. Independently classified particles from each FAS preparation were categorized based on conformation of top and bottom portions of the structure and the percentage of particles presenting each conformation was determined. Bars are colored as in a and b.

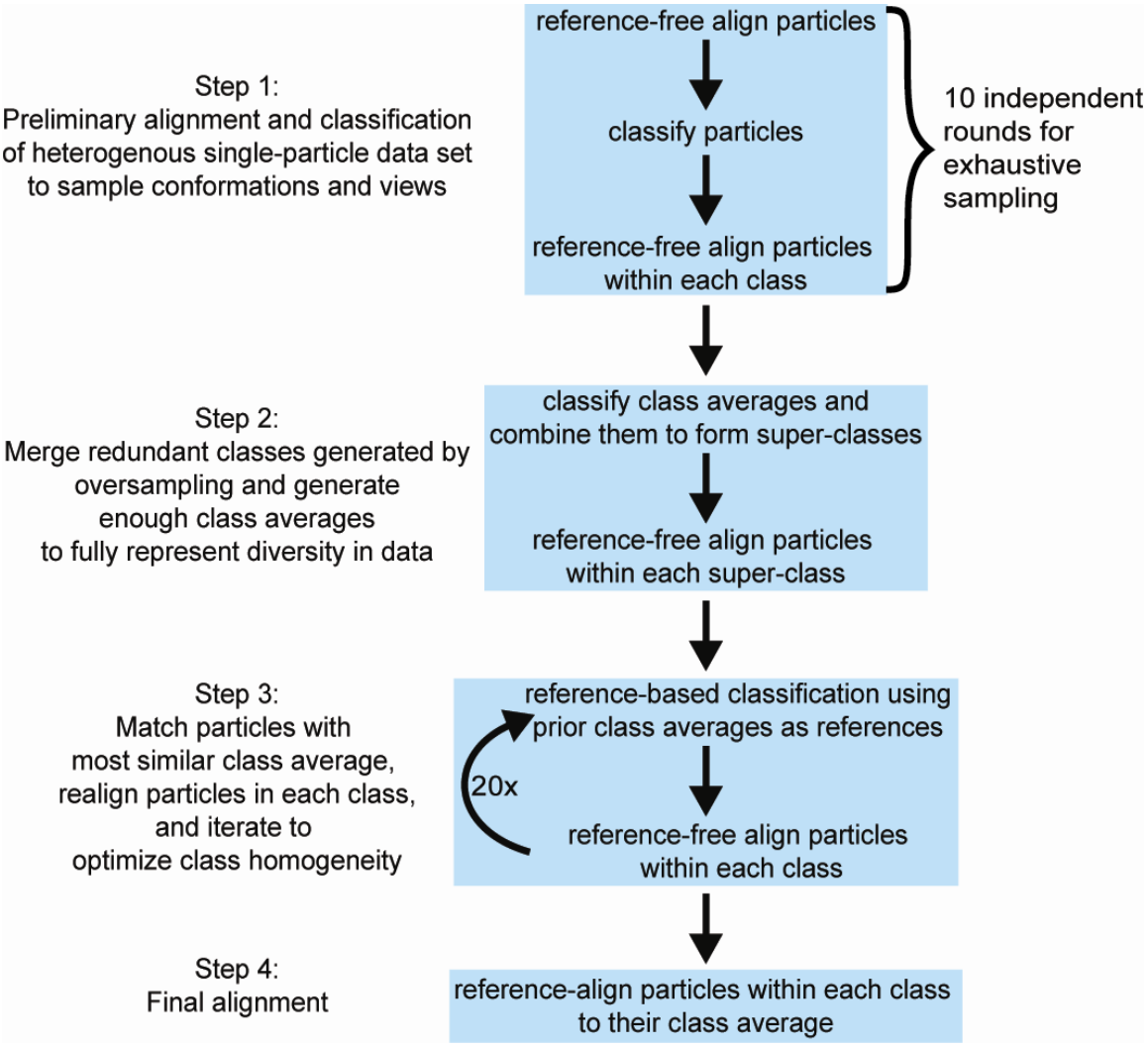

Supplementary Figure 5 Outline of procedure for alignment and classification of single-particle images. (Step 1) To avoid reference-biased alignment of images we initiated our procedure with a reference-free alignment and classification module. As the alignment of heterogenous images generally produces variable results[5] this alignment/classification module was repeated 10 times to ensure broad sampling of particle alignments. Finally reference-free alignment was performed within these more homogenous classes of particles. (Step 2) Since similar classes often result from these alignment and classification rounds, a second classification of the class averages was performed to reduce this oversampling. Then particles were again reference-free aligned within these super-classes. The number of classes at this step was determined based on the heterogeneity of the specimen and the desired number of particles to obtain useful resolution of details in the resulting class averages and RCT reconstructions. (Step 3) These super-class averages were used to initiate 20 cycles of supervised classification and alignment permitting particles to change their class assignment based on similarity to class averages from the prior cycle. Finally particles within each class were aligned directly to their class average.

Supplementary Movie 1 2D analysis reveals a continuum of domain rearrangements within the β-carbon processing portion of FAS. Conformational changes within the upper portion of the structure were better defined by restricting the 2D particle alignment and classification to this region of the structure. This was accomplished by applying a soft edged mask to isolate the upper domains in the particle images after initial whole particle alignment/classification to orient the images. After alignment of the masked particles, alignment parameters were applied to the unmasked particles, resulting in a blurring of the lower portion of the structure that was excluded from the alignment, while structures become better defined in the upper portion. Using these particles with an optimal alignment of the upper portion of the structure classification was focused on the β-carbon processing domains. During focused classification it was apparent that the first eigenimage accounts for the majority of the variance. Since this first classification factor was very dominant, class averages could be placed into a linear sequence for animation according to their first eigenvalue. 73 of the 100 class averages were used for this animation, which is looped in the forward and reverse directions.

Supplementary Movie 2 An animation illustrates how FAS may interchange between the experimentally observed conformations to facilitate contacts between the ACP and active sites of the catalytic domains in a typical reaction cycle. Atomic models were fitted into four 3D EM reconstructions (**Fig. 3**, #888, #823, #706, and #1103) that would suffice to enable domain interactions required for fatty acid synthesis. To generate the animation, intermediate structures were generated and sequentially displayed in Chimera[6] with each chamber completing about two chain extension and processing cycles. The ACP and TE domains were omitted for clarity. The range of motion of each ACP is indicated by a transparent gray sphere. As an active site comes within reach of an ACP (or becomes accessible to it in the case of the ER domains) the phosphopantetheine ligand appears in red with its point of attachment to the ACP marked by a sphere colored to match the enzyme being contacted. The animation starts with the subunits arranged in the crossed-over configuration and chain extension within the left chamber is initiated by the transfer of a saturated acyl moiety (containing from 2 to 14 carbon atoms) from the ACP to the KS. A swinging motion allows the ACP in the left chamber to collect a malonyl moiety from the MAT of the opposite subunit and engage in a condensation reaction with the KS of the same subunit. These motions are orchestrated with rolling motions of the DH and ER dimers in the upper portion of the structure that obstructs the ER active site in the left chamber while making the ER active site more accessible in the right reaction chamber. As a result of the rolling motion the series of β-carbon processing reactions in the right chamber, which follow chain extension reactions that would have transpired prior to the start of the movie, occurs simultaneously with catalytic events in the left chamber. The lower portion of the structure then swings to the opposite side facilitating chain extension reactions in the right chamber synchronized with β-carbon processing reactions in the left chamber. An optional swiveling motion switches the subunits to the back-to-back configuration allowing the same series of reactions in the two chambers except that the ACP domains contact the MAT of the same subunit and the KS of the opposite subunit.

This interpretation of FAS dynamics and catalysis could be an oversimplification, for instance β-carbon processing could also be accomplished in a closed chamber if the DH and ER were in the accessible asymmetric conformation (as in **Fig. 3**, #691). Therefore this animation represents a minimal set of motions that could explain all available biochemical and structural information and reflects one of several combinations of the observed conformations and enzyme reactions.

REFERENCES

1. Joshi, A.K., Witkowski, A., Berman, H.A., Zhang, L. & Smith, S. Effect of modification of the length and flexibility of the acyl carrier protein-thioesterase interdomain linker on functionality of the animal fatty acid synthase. *Biochemistry* **44**, 4100-7 (2005).
2. Chakravarty, B., Gu, Z., Chirala, S.S., Wakil, S.J. & Quiocho, F.A. Human fatty acid synthase: structure and substrate selectivity of the thioesterase domain. *Proc Natl Acad Sci U S A* **101**, 15567-72 (2004).
3. Rosenthal, P.B. & Henderson, R. Optimal determination of particle orientation, absolute hand, and contrast loss in single-particle electron cryomicroscopy. *J Mol Biol* **333**, 721-45 (2003).
4. Maier, T., Leibundgut, M. & Ban, N. The crystal structure of a mammalian fatty acid synthase. *Science* **321**, 1315-22 (2008).
5. Penczek, P., Radermacher, M. & Frank, J. Three-dimensional reconstruction of single particles embedded in ice. *Ultramicroscopy* **40**, 33-53 (1992).
6. Pettersen, E.F. et al. UCSF Chimera--a visualization system for exploratory research and analysis. *J Comput Chem* **25**, 1605-12 (2004).